Living on the Edge: Unequal Rise of Global Population Exposure on Steep Terrain

Chakshu Gururani[1], Ugur Ozturk[2], Thorsten Wagener[1]

Author One: https://orcid.org/0009-0000-6038-0234
Author Two: https://orcid.org/0000-0002-7641-4344
Author Three: https://orcid.org/0000-0003-3881-5849

[1]Institute for Environmental Science and Geography, University of Potsdam, Potsdam, Germany
[2]Department of Geography and Regional Research, University of Vienna, Vienna, Austria

This manuscript is a non-peer-reviewed preprint submitted to EarthArXiv.

Living on the Edge: Unequal Rise of Global Population Exposure on Steep Terrain

This manuscript is a preprint and has not been peer reviewed.

Chakshu Gururani[1*], Ugur Ozturk[2] and Thorsten Wagener[1]

[1*] Institute for Environmental Science and Geography, University of Potsdam, Potsdam, Germany .

[2] Department of Geography and Regional Research, University of Vienna, Vienna, Austria .

*Corresponding author(s). E-mail(s): chakshu.gururani@uni-potsdam.de;

Abstract

Population growth on steep terrain can increase exposure to slope-related hazards, yet its global distribution and socioeconomic context remain poorly understood. To characterize this exposure using a globally consistent topographic measure, we analyse 1-km gridded population and settlement data on terrain with slope inclination $\geq$ **10°** from 1975–2025, and aggregate selected metrics to topographic catchments (mean area ∼10,000 km^2) for spatial comparison. We find that the steep-terrain population increased from approximately 494 to 835 million people, and that this growth was highly unequal across regions and socioeconomic settings. The largest increases occurred in tropical regions, with prominent hotspots in the Kivu Rift, southern Yemen, the Hindu Kush and Southeast Asia. Low- and lower-middle-income countries accounted for more than half of the global increase. Low-income countries had the highest share of their population living on steep terrain in 2025, at 18%, compared with 6.4% in high-income countries. The changing settlement patterns were also reflected in substantial peri-urban growth on steep terrain, particularly in Sub-Saharan Africa and South Asia. Major hotspots of steep-terrain population growth experienced substantial land-cover change and largely overlapped with areas of high landslide susceptibility identified using an independent global dataset. Our results provide a globally consistent baseline for identifying where growing populations on steep terrain coincide with broader patterns of settlement and environmental change relevant to hazard monitoring and risk-informed planning.

Keywords: population exposure, rapid urbanization, steep terrain, landslides

Introduction

Global population exposed to natural hazards roughly doubled from about 1.9 to 4 billion between 1975 and 2015 [1]. Additionally, today nearly 90 million, three-quarters of all displaced people, live in regions classified as highly or extremely hazard-prone [2, 3]. Many of these regions are located in the tropics [2], where limited data often constrain the evaluation of physical hazards and human exposure [4, 5], especially on poorly accessible steep and unstable terrain [6].

While progress has been made in assessing exposure to major hazards such as floods or tropical cyclones, multiple IPCC reports highlight global landslide assessments to be often limited to coarse scales [7, 8]. This gap arises from three related reasons. (i) Impacts are usually recorded only after major events [9–11], resulting in damage being captured mainly in well-studied or more populated areas. (ii) Many global studies rely heavily on inventories or case-specific observations [12, 13]. (iii) Limited and biased data constrain global assessments and models. Consequently, the global distribution of landslide hazards and exposure remains unevenly mapped, with major gaps in many mountainous and rapidly developing regions [14]. Landslides are therefore rarely included in global multi-hazard risk assessments that increasingly explore how climate extremes and hazard exposure are changing [15, 16].

Several recent studies have advanced global and national assessments of landslide exposure, but none explicitly tracked how exposure evolves as populations and settlements redistribute across steep terrain. National income and land-cover change have been shown to govern landslide impacts at the country scale, without resolving local settlement patterns or sub-national variation in exposure [17]. Exposure to large, slow-moving, deep-seated landslides in cities has more than doubled since 1985 [18], leaving open how this exposure varies by settlement type. "Slope climbing" due to global urban expansion has been quantified [19], showing that cities increasingly expand onto steeper slopes, yet how this pattern extends to population growth in rural and peri-urban settings remains to be explored. Global estimates of exposure to rainfall-triggered landslides have also been developed using modelled hazard conditions for 2001–2019 [20], including annual and seasonal variability in exposure. However, these estimates rely on essentially static population and infrastructure data and therefore do not resolve how population and settlement distributions on steep terrain have changed over several decades.

Both physical and human systems are changing, shifting locations where landslide instability intersects with population growth [14, 21]. Rainfall extremes are intensifying in many regions [22, 23], which can change and expand the areas prone to rainfall-triggered landslides [24–27]. In parallel, settlement growth is pushing into steeper terrain through land-use change [28], deforestation [29] and the expansion of both formal and informal settlements [30, 31]. Differences in income, infrastructure and

governance influence settlement patterns, safety standards, and the capacity to adapt [8, 32, 33]. As a result, landslide exposure is changing.

Although global landslide exposure is increasingly discussed, its dynamics remain under-explored especially below the country scale. Because available landslide inventories and hazard data are neither spatially complete nor temporally consistent worldwide, we measure population change on steep terrain as a globally consistent first-order screening indicator of where populations are increasingly located on terrain potentially relevant to landslide susceptibility. We define steep terrain as areas with slope angle $\geq 10°$ because slope is a primary control on landslide susceptibility and explains a substantial share of its spatial variation [34]. We ask two questions: where did population growth occur on steep terrain, and which settlement types, for example urban centres, peri-urban areas, or rural settlements, accounted for this growth across regions? We combine gridded population data at 1-km resolution [35] from 1975–2025 with slope data at 250-m resolution [36]. We also aggregate the total and average results at HydroBASINS Level 5 catchment level [37], with a mean area of approximately 10,000 km^2. The threshold provides a transparent basis for comparison across regions and through time, but does not capture all controls on landslide susceptibility or triggering. We therefore also test alternative slope thresholds, compare steep-terrain population-growth patterns with an independent global susceptibility product [38], and examine extreme-rainfall intensity to provide additional context on potential triggering conditions [39]. We additionally compare population change and population-density change on steep and non-steep terrain within individual catchments, distinguishing large absolute additions on steep terrain from population growth that is disproportionately concentrated there, and examine associated land-cover transitions. Finally, we assess how steep-terrain population change varies across settlement types, climate zones, income levels, and political stability. Our approach complements recent global studies on landslide exposure while adding a multi-decadal view of where population on steep terrain increased and under which development contexts.

Results

Tropical climates dominate in steep-terrain population growth

Overall population growth is heterogeneous across global mountain belts, but its convergence with steep terrain is concentrated in distinct regional clusters (Figure 1). Several of these clusters are in regions that are inconsistently highlighted in event-based global assessments, such as the Ethiopian Highlands and the Southern Levant [9, 12]. Steep terrain and rapid population growth thus converge in several climate zones. We use the 1 km gridded population and settlement data from the Global Human Settlement Layer (GHSL) datasets [35, 40] and climate zones from the IPCC Climate Zone Map, derived from long-term monthly temperature and precipitation data (1901–2019) [41]. The classification distinguishes 12 climate zones based on temperature, moisture conditions and elevation, including distinct Tropical Wet, Tropical Dry classes and so on. Each catchment is assigned its dominant climate class (see Materials Section).

We find the highest Compound Annual Growth Rates (CAGR) of steep-terrain population in tropical montane regions (∼2.3% yr^{-1}), more than tripling from 42 million people in 1975 to 128 million in 2025. Tropical wet (∼1.9% yr^{-1}) and dry (∼1.8% yr^{-1}) climates also have growth rates higher than the global average (∼1.1% yr^{-1}), with populations on steep terrain rising from 28 to 70 million and from 16 to 39 million, respectively. In absolute terms, the largest additions to steep-terrain population occurred in tropical montane (+86 million), followed by warm temperate dry (+68 million) and tropical moist climates (+61 million).

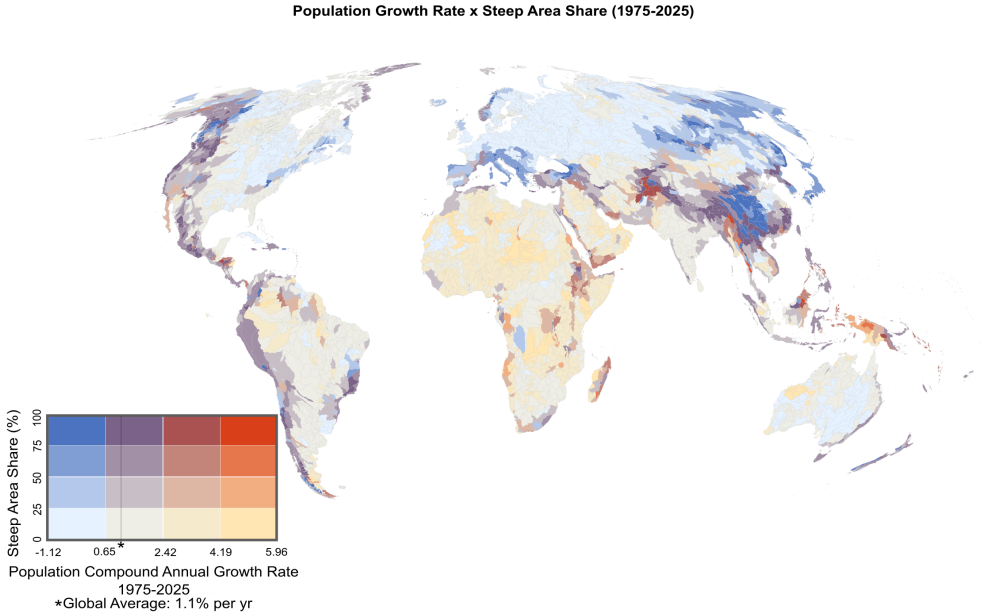


Fig. 1 Population growth and steep-terrain extent, 1975–2025. Bivariate map showing the overall catchment population Compound Annual Growth Rate (CAGR; x-axis of legend) and the share of each catchment classified as steep ($\geq 10°$; y-axis of legend). Reddish hues indicate catchments where high overall population growth coincides with a large share of steep terrain.

Although the global population living on steep terrain increased from 494 to 835 million between 1975 and 2025, its share of the total population declined from 12% to 10.2%. This contrast indicates that population growth is not uniformly shifting towards steeper terrain worldwide. Instead, faster relative growth on steep than on non-steep terrain is regionally concentrated. Only 147 of the 5,393 analysed catchments, approximately 3%, had greater net population change on steep terrain than on non-steep terrain (Supplement S2). These catchments nevertheless accounted for approximately 15% of the global net increase in steep-terrain population. They were strongly concentrated in mountainous settings, with a mean steep-terrain area share of 65% and mean catchment slope of 17°, compared with 15% and 5°, respectively, in the remaining catchments. Geographically, examples occur in parts of the Ethiopian Highlands, around the Kivu Rift, in the Hindu Kush–Himalayan region, parts of China,

Central America and Papua New Guinea among others (Supplement Figure S2a). Many also coincide with the major global hotspots of absolute steep-slope population increase, indicating that this pattern is not restricted to small catchments with modest growth.

We also conducted a within-catchment analysis comparing net population change and population-density change on steep and non-steep terrain (Supplement S3). 31% of the catchments showed greater population and density change on non-steep terrain, while 32% showed similar increases in both population and population density on steep and non-steep terrain. In contrast, only 34 catchments (1%) showed greater change on steep terrain in both population and population density. 5% had greater population change on steep terrain but similar density change, while 72 (2%) had greater density change on steep terrain without greater absolute population change. Overall, 8% of valid catchments showed steep-terrain dominance in at least one of the two measures.

Steep-terrain population growth is predominantly concentrated in lower-income regions with greater land-cover change

The top 10 hotspots identified in our analysis, defined as the catchments with the largest absolute increases in population on steep terrain, are located in low- or lower-middle-income countries (Figure 2). The largest steep-terrain population increases were also unevenly distributed across income groups. Low- and lower-middle-income countries account for about 56% of the absolute population growth on steep terrain between 1975 and 2025. Using the latest World Bank income-group classification, our results show that the population on steep terrain grew by about 114 million in lower-middle-income countries and by about 83 million in low-income countries. Major hotspots in these groups include the Kivu Rift, southern Yemen and Afghanistan in low-income countries, and Pakistan and the Philippines in lower-middle-income countries. Other hotspots occur in upper-middle-income countries, including Peru, Indonesia and China. Over the same period, steep-terrain population grew by about 10 million in high-income countries and by about 61 million in other or unclassified countries. The unclassified category includes Ethiopia, where the Ethiopian Highlands form another major region of steep-terrain population growth. Moreover, low-income countries had the highest share of their total population living on steep terrain in 2025 (18%), whereas the lowest share was observed in high-income countries (6.4%) (Supplement Section S12).

Several of the largest increases in population on steep terrain occur in politically fragile regions. For example, major hotspots include southern Yemen (+7.5 million), the Hindu Kush region (+7 million), and Java, Indonesia (+6.37 million). Many are in countries that rank near the bottom of the World Bank 'Political Stability and Absence of Violence' index (Supplement Section S7). The index reflects perceptions of political instability and politically motivated violence, including terrorism, and is reported as a rank from 1 to 100, where 1 indicates the lowest political stability and 100 the highest. Several associated countries also rank low in political stability, including Yemen (rank 1), Ethiopia (rank 6), Pakistan (rank 7), and Burundi (rank 13).

The largest single increase occurred in the region surrounding Lake Kivu, a tropical montane and low-income region where the population living on steep terrain increased

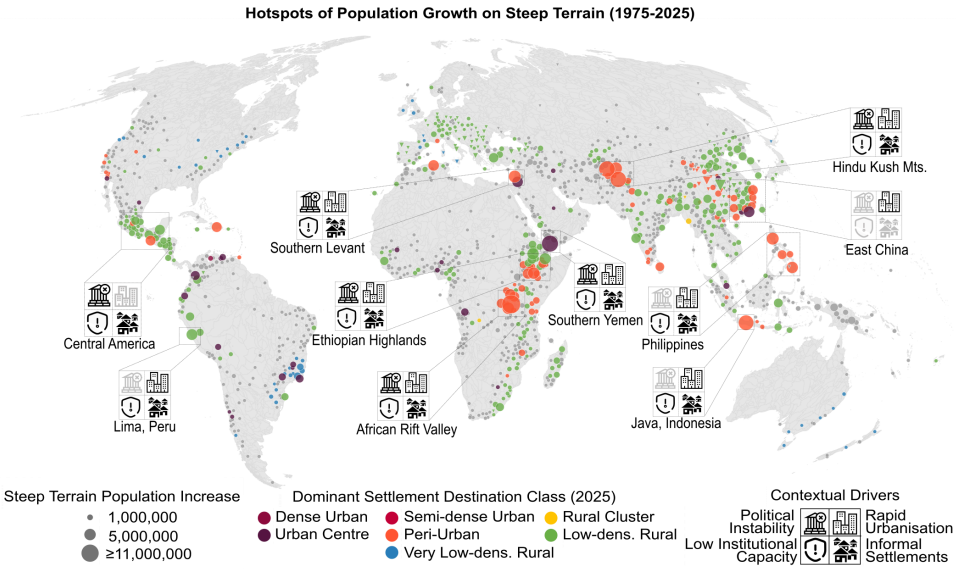


Fig. 2 Steep-slope population change and dominant settlement patterns, 1975–2025. Map shows the absolute increase in population living on steep terrain ($\geq 10°$) per catchment, with point size scaled to total growth and colour indicating the dominant GHS-SMOD settlement class in 2025. Labelled regions highlight where steep-slope exposure intersects with different settlement patterns and contextual drivers including political instability, low institutional capacity, rapid urbanisation and informal settlement expansion (definitions in Supplement Section S6). Contextual drivers, excluding political instability, are based on regional landslide-risk studies in those hotspots, mentioned in the Discussion (details in Supplement Section S8). Extracted from published case studies, contextual drivers may not represent the entirety of the study period. Inverted triangles represent population decrease on steep terrain.

by about 10 million between 1975 and 2025 (Figure 2). Catchments in this region also show both net population change and population-density change to be greater on steep than on non-steep terrain. This region lies on the western flank of the East African Rift and experiences frequent landslides [42]. It is also affected by persistent political instability [29].

These high-growth catchments also showed greater forest loss, cropland expansion, and built-up expansion. To quantify these changes, we used the HILDA+ land-use and land-cover dataset [43], comparing land-cover between 1975 and 2019 and calculating, for each catchment, the share of area undergoing forest loss, cropland expansion, pasture expansion, and built-up expansion. The 100 catchments with the largest absolute steep-terrain population increases showed a greater mean share of catchment area undergoing forest loss (about 5.2% vs. 2.9%), cropland expansion (4.8% vs. 2.2%), and built-up expansion (1.1% vs. 0.5%) than the remaining catchments (Figure 3).

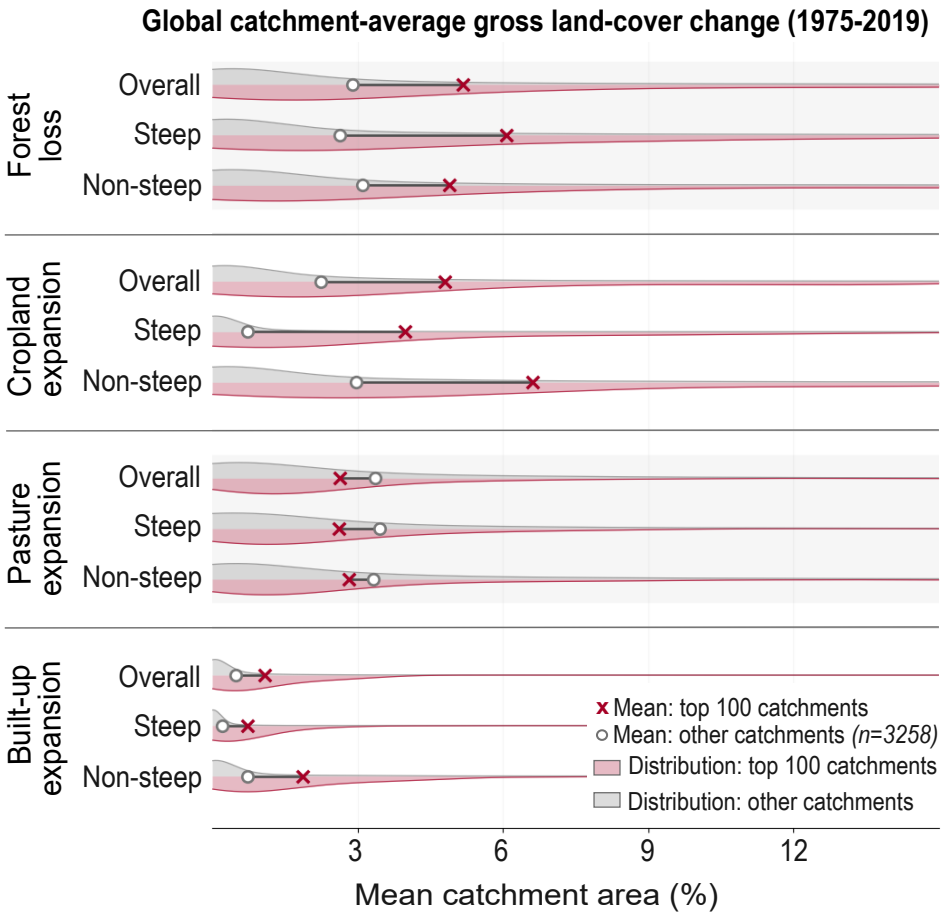


Fig. 3 Catchment-average gross land-cover change in the 100 catchments with the largest absolute steep-terrain population increases compared with all other catchments, 1975–2019. Gross forest loss, cropland expansion, pasture expansion, and urban expansion were derived from HILDA+ land-cover transitions and calculated as the percentage of catchment area undergoing each transition. Results are shown for the whole catchment and separately for steep and non-steep terrain. Crosses indicate the mean for the Top 100 catchments, circles indicate the mean for the remaining catchments, and shaded distributions show variation among individual catchments.

These contrasts were also evident on steep terrain, where the mean share of steep-terrain area undergoing forest loss was about 6.1% in the Top 100 compared with 2.6% in the remaining catchments between 1975 and 2019, while the corresponding values were 4.0% vs. 0.7% for cropland expansion and 0.7% vs. 0.2% for built-up expansion. Pasture expansion differed from this pattern and was lower in the Top 100. Together, these results indicate that the largest increases in population on steep terrain occurred within catchments undergoing broader demographic and land-cover change. The type and magnitude of land-cover change associated with these hotspots also differed across

income groups, with particularly strong forest-loss and cropland-expansion contrasts in low- and lower-middle-income countries (Supplement Section S5).

Rapid urbanization is reshaping where people live

To better understand how steep-terrain population growth is distributed across settlement types, we quantified how the population living on steep terrain is distributed across the seven GHS-SMOD settlement classes (including urban center, peri-urban, etc.) between 1975 and 2025 (Figure 4) (see Materials Section for details). Absolute steep-terrain population growth was the largest in Sub-Saharan Africa (+98 million) and East Asia & the Pacific (+82 million), followed by Latin America and the Caribbean (+58 million) and South Asia (+50 million), while Europe (+1 million) and North America (+4 million) changed only modestly.

Our results show a shift of steep-slope population towards peri-urban and urban classes between 1975 and 2025. Globally, peri-urban steep-slope population increased from 70 million to 179 million (+109 million), and urban-centre steep-slope population increased from 68 million to 183 million (+115 million). The peri-urban shift was strongest in South Asia and Sub-Saharan Africa, where the share of steep-slope population living in peri-urban areas more than doubled, from 15% to 31% and from 13% to 32%, respectively. Over the same period, the share of global steep-terrain population in very low-density rural areas decreased from 9% to 5%. We also analysed changes in the share of each settlement class located on steep terrain and found the highest increases in steep-area share for peri-urban and semi-dense urban classes in several regions (Supplement Section S1). The increasing representation of peri-urban and semi-dense populations on steep terrain is consistent with the concept of 'slope climbing' observed in global urban expansion [19]. Similar expansion into peripheral and steep areas has been documented in cities worldwide: built-up area on inhabited large landslides doubled across 129 cities between 1985 and 2015 [18], while in Medellín, Colombia, landslide impacts increasingly affected newly developed peripheral neighbourhoods [44]. Informal settlement on such slopes can further increase landslide occurrence, as shown for Saint Lucia [30].

Steep-population-growth hotspots overlap with landslide susceptibility mapping

The steep-terrain metric identifies where population growth occurred on slopes $\geq 10°$, but it does not represent a complete landslide-susceptibility model. To assess potential differences, we compared our slope-based results with the global susceptibility product of Stanley and Kirschbaum (2017) [38]. This comparison allowed us to assess how much susceptible terrain and associated population growth would be retained if 'High' and 'Very High' susceptibility classes were used instead of the fixed slope threshold.

Our $\geq 10°$ definition captures about 97% of all terrain classified as High or Very High susceptibility. Of the remaining High—Very High susceptibility terrain below 10°, about 90% lies immediately adjacent to terrain with 10° slope angle. Even the excluded area is generally not flat, with a median slope angle of 8.2°, an interquartile range of 6.5°–9.2°, and 87% occurring on slopes of at least 5°. However, High–Very

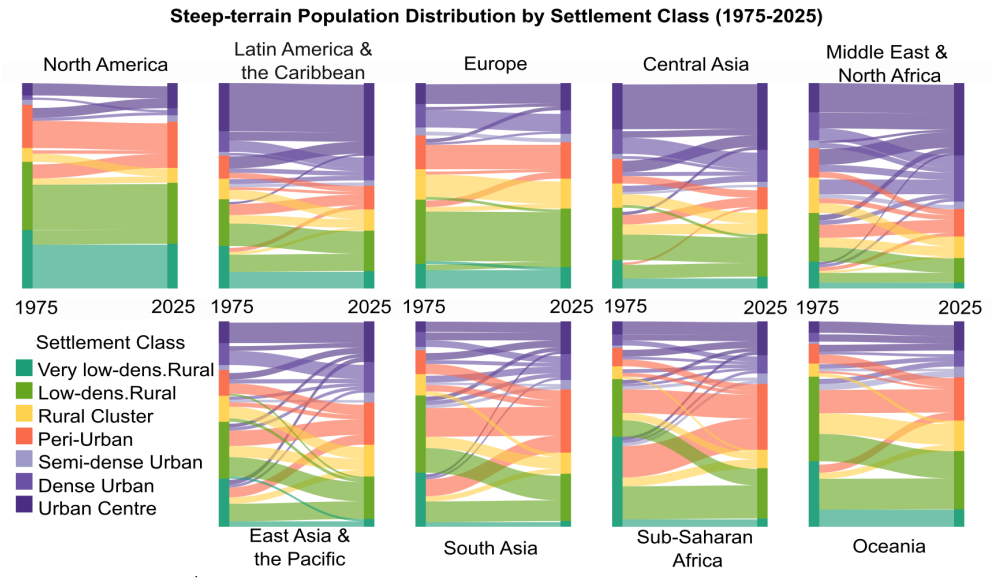


Fig. 4 Change in population distribution across settlement classes on steep terrain ($\geq 10°$), 1975–2025. The figure shows the share of the steep-terrain population across GHS-SMOD settlement classes. Most regions show increasing shares in peri-urban and urban classes over time, with notable rural-to-urban transitions in Sub-Saharan Africa and East Asia & the Pacific. The full 5-year stepwise transitions are shown in Supplement Section S4.

High susceptibility terrain accounts for 45% of the total area selected by the slope threshold, indicating that the slope definition forms a broader screening envelope that also includes Moderate and lower susceptibility classes.

Approximately 90% of both slope-defined terrain and its associated positive population growth occurs within Moderate, High or Very High landslide-susceptibility classes. The main hotspot geography also remains similar when the fixed slope threshold is replaced by High–Very High susceptibility: 39 of the top 50 catchments appear in both rankings, with a strong correlation in catchment rankings (Spearman $= 0.87$). These results indicate that the principal population-growth hotspots are broadly retained under an independent susceptibility classification, and the slope-based definition provides a broader screening measure of potentially susceptible terrain..

To provide context on potential triggering conditions, we used the BURGER dataset [39], which provides globally regionalised rainfall intensity–duration–frequency (IDF) estimates derived from rain-gauge observations and statistical modelling. We selected the estimated rainfall intensity for a six-hour storm with a 100-year return period and summarised it using the 90th percentile within each catchment (see Materials Section). Among the 50 catchments with the largest positive population increases on terrain 10°, 47 had rainfall intensities above the global catchment median and 46 had an above-median proportion of steep terrain classified as High or Very High susceptibility. Forty-three catchments exceeded both medians (Supplement Section S10). These results indicate that many leading steep-terrain population-growth hotspots

coincide with relatively high estimated extreme-rainfall intensities and substantial mapped susceptibility. Rainfall intensity is used here as physical context and is not interpreted as landslide frequency or observed landslide occurrence.

Discussion

Interpreting steep-terrain population growth in the absence of complete landslide data

Our findings extend previous global assessments of landslide exposure by reconstructing multi-decadal changes in population distribution on steep terrain. While earlier work has examined landslide impacts across income and land-cover conditions [17], exposure to large landslides in cities [18] and global rainfall-triggered landslide exposure [20], our analysis identifies where population growth on steep terrain has occurred across different settlement types and regional contexts. We found that most steep-terrain population growth accompanied broader catchment population expansion, while disproportionate growth on steep terrain was limited to a small subset of catchments. However, catchments undergoing stronger growth on non-steep terrain still have added millions of people on steep terrain. Absolute growth and disproportionate steep-terrain growth therefore describe different dimensions of changing exposure. This distinction is important because a large increase in exposed population does not necessarily imply a preferential shift towards steeper locations.

Interpreting these patterns in relation to landslides is challenging because global inventories and impact records remain spatially incomplete and temporally inconsistent [14, 34]. For example, the Kivu Rift—spanning parts of the Democratic Republic of the Congo, Rwanda and Burundi—is a well-documented landslide hotspot, with regional inventories identifying thousands of shallow landslides and frequent casualties [e.g., 29, 42]. Yet its prominence can be underestimated in global assessments that rely on event databases such as EM-DAT [9], whose coverage and recorded impacts are shaped by inclusion thresholds, reporting capacity and uneven reporting [11, 45]. We also identified an increase of about 60 million people on steep terrain in regions not assigned to a World Bank income group, including parts of the Ethiopian Highlands. Thus, despite strong regional evidence [17], some rapidly changing regions may remain poorly represented in global assessments based on available event data [13].

To reduce dependence on these uneven records, we used globally consistent gridded population and slope data. The $\geq 10^{\circ}$ threshold should be interpreted as a first-order screening indicator of steep-terrain exposure, rather than as a complete measure of landslide susceptibility, hazard, or risk. Although steepness is a primary control on landslide susceptibility [34], it is less informative where instability is dominated by geology, soils, land cover, drainage, or engineered slope modification [46–49]. The sensitivity analysis nevertheless shows that differences among income groups persist as the threshold is increased (Supplement Section S12), indicating that the broad pattern is not driven by a single cutoff.

The comparison with Stanley and Kirschbaum shows that this simple threshold nevertheless performs reasonably well as a broad global screening measure. Nearly 97% of the High–Very High susceptibility terrain is captured by the threshold, and

most of the small amount lying below 10° occurs immediately adjacent to steeper terrain. This result partly reflects the continuous nature of topography and the approximately 1-km resolution of the susceptibility product, although local geological and anthropogenic controls may also be important. For example, geological and tectonic conditions have shown to influence landslide susceptibility along the Karakoram Highway in Pakistan [48], while urban expansion and terrain modification affect landslide activity in Medellín, Colombia [44].

The rainfall comparison adds a complementary measure of potential landslide-triggering conditions to the susceptibility assessment. Previous studies have highlighted the importance of rainfall intensity for landslide occurrence and the challenges of representing these conditions consistently across regions [20, 25, 26]. Our results show that many leading steep-terrain population-growth hotspots coincide with relatively high estimated six-hour, 100-year rainfall intensities and substantial mapped susceptibility (Supplement Section S10). However, the BURGER estimates are derived from regionalised rainfall statistics and remain uncertain where gauge coverage is sparse [39]. They provide context for potential triggering conditions but do not demonstrate that landslide frequency or rainfall intensity increased between 1975 and 2025.

The susceptibility product also contains assumptions and uncertainties of its own. Stanley and Kirschbaum (2017) combine slope, geology, faults, roads, and forest loss using a heuristic fuzzy model, and note that global classifications may perform differently when applied to local settings [38]. For example, their discussion of Indonesia notes that Java appears less hazardous than neighbouring islands despite its large number of reported landslides, potentially reflecting inventory bias or anthropogenic terrain modification. This illustrates why a susceptibility product should not be treated as an error-free reference against which the slope metric is judged. A transparent slope threshold provides a consistent alternative that minimises dependence on regionally variable model assumptions, while the susceptibility comparison indicates where that simplification is well supported and where it requires caution.

Steep-terrain population growth is concentrated in lower-income, peri-urban and rapidly changing settings

Our findings show that low- and lower-middle-income countries accounted for approximately 198 million of the 341 million net increase in steep-terrain population between 1975 and 2025. The largest increases occurred in tropical regions of Asia, Africa, and South America. Many of these regions remain under-represented in landslide–climate research [14] and in natural-hazard research more broadly [4, 5]. This research gap is important because rainfall extremes are projected to intensify in many of these regions [22, 25]. For example, projected increases in extreme precipitation may intensify landslide activity in parts of High Mountain Asia, including mountainous areas near glaciers and glacial lakes [25]. Our comparison with the BURGER rainfall intensity dataset [39] further shows that many of the largest steep-terrain population-growth hotspots already coincide with relatively high present-day estimated six-hour, 100-year rainfall intensities and substantial mapped landslide susceptibility. Although

BURGER does not represent temporal changes in rainfall, this spatial correspondence highlights regions where growing populations on steep terrain may warrant more detailed landslide assessment.

The largest increases in steep-terrain population occurred alongside peri-urban and semi-dense urban expansion (Figure 2). Between 1975 and 2025, the share of steep-terrain population living in peri-urban areas more than doubled in Sub-Saharan Africa, from 13% to 32%, and in South Asia, from 15% to 31%. Peri-urban areas are often characterised by rapid land conversion, stretched infrastructure, fragmented governance, and limited land-use control [50]. These conditions may allow settlement expansion to outpace hazard assessment, infrastructure provision, and planning.

The land-cover analysis reinforces this picture of broader landscape transformation. Catchments with the largest absolute increases in steep-terrain population experienced greater forest loss, cropland expansion, and built-up expansion than other catchments, including on steep terrain (Figure 3). This observation is consistent with the within-catchment population analysis, which shows that many of the largest steep-terrain growth hotspots are also undergoing substantial population growth on non-steep terrain. These findings complement previous evidence that land-cover change and socioeconomic conditions are associated with landslide impacts [17], while land-use modifications can also influence slope instability [46]. Our analysis adds a spatial exposure perspective by showing that the catchments with the largest steep-terrain population increases are also experiencing comparatively strong landscape transformation.

High-income regions experienced much smaller increases in steep-terrain population. This contrast may reflect differences in demographic growth, planning capacity, infrastructure, housing markets, and the availability of buildable land [19, 44]. Our analysis does not isolate the contribution of these factors, but it shows that rapid steep-terrain population growth is concentrated in regions where monitoring, planning, research, and reporting capacity may also be limited [5].

Urban expansion can disproportionately affect lower-income households and vulnerable communities, which are often more likely to occupy hazardous land with limited planning oversight [50, 51]. For example, in Latin America and the Caribbean, 81% of landslide fatalities between 2004 and 2013 occurred in poor or informal settlements, although such settlements accounted for only 41% of recorded fatal landslide events [52]. In Medellín, Colombia, long-term urban expansion into peripheral areas has been closely coupled with landslide occurrence, illustrating how city growth can progressively place new neighbourhoods in hazardous terrain [44]. In Bujumbura, Burundi, rapid and largely unplanned expansion into unserviced areas has been associated with widespread flood, flash-flood and gully impacts, reflecting weaknesses in drainage, infrastructure and urban governance [53]. In Lima, Peru, unequal access to safe land, housing and basic services has been identified as a central driver of socially constructed disaster risk [54], while on the North Coast of São Paulo, Brazil, rapid urban growth and spatial segregation concentrated the impacts of the 2023 disaster in lower-income neighbourhoods [55]. Comparative evidence from Freetown, Antipolo, Baguio, Port-au-Prince and Bukavu similarly shows that informal settlements tend to

occupy steeper and more landslide-exposed terrain than more formally planned neighbourhoods [31]. Together, these studies show that steep-terrain settlement can emerge through different combinations of urban expansion, land scarcity, housing constraints, unequal service provision and informal development.

These findings suggest that steep-terrain exposure develops through interactions among settlement expansion, physical terrain constraints, and wider institutional and socioeconomic conditions. Based on the hotspot case studies, we summarise these possible interactions in a conceptual framework (Figure 5).

We identify where population change on steep terrain occurred, not why individual households or settlements occupied particular locations. Land prices, agricultural livelihoods, proximity to employment, infrastructure development, land scarcity, historical settlement patterns, and informal expansion may all contribute [29, 31, 56, 57]. Similar spatial outcomes may therefore emerge through different development pathways, and the observed global pattern cannot be attributed to a single driver.

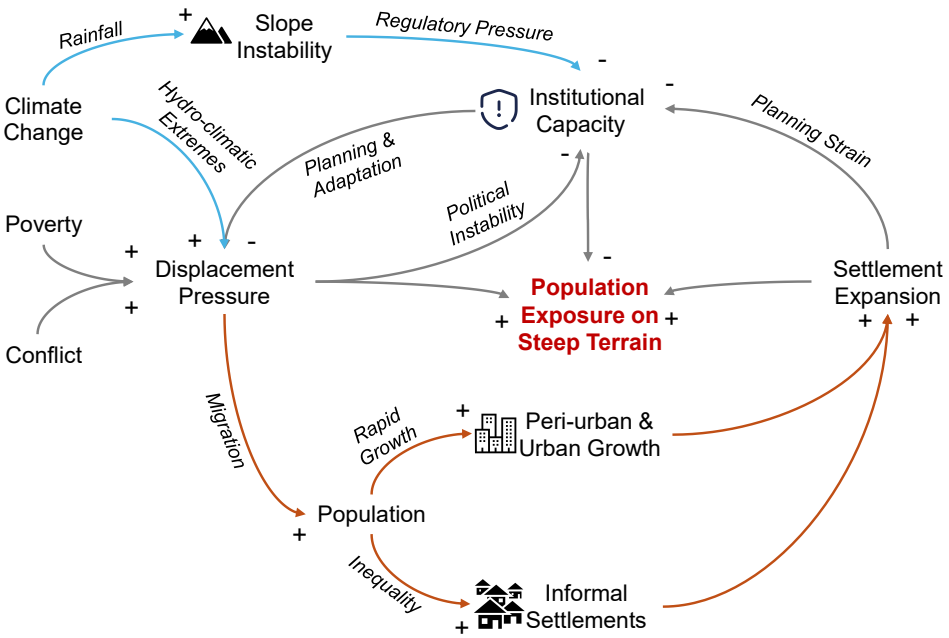


Fig. 5 Conceptual framework informed by regional case studies of the identified hotspots. Diagram of interacting processes and contextual factors associated with population exposure on steep terrain. Arrows indicate plausible pathways identified across the case studies. (+)/(−) denote positive and negative effects. The blue pathways represent climatic controls on slope instability and displacement, while the brown pathways represent population and settlement processes associated with expansion onto steep terrain. The diagram synthesises the regional cases and contextual definitions provided in Supplement Section S8 for the hotspots identified in Figure 2.

Many hotspots also face wider socioeconomic and multi-hazard pressures

Hotspots in the Hindu Kush, the Kivu Rift, Southeast Asia, and Central America also face multiple pressures, including conflict, political instability, land scarcity, displacement, and other natural hazards [2, 3]. Many of the associated countries rank near the bottom of the World Bank's 'Political Stability and Absence of Violence' index. Rapid steep-terrain population change in these regions therefore occurs within wider social and institutional pressures. There is growing evidence that climate hazards can interact with competition over resources and existing social tensions [58, 59]. In such cases, landslides may be only one among several immediate concerns. Violence, displacement, food insecurity, housing shortages, and loss of livelihoods may influence settlement patterns more directly than geomorphological risk alone [29, 33, 60].

Settlement on steep terrain should therefore not be interpreted simply as a deliberate choice to occupy hazardous land. Different regional pathways can produce similar patterns of steep-terrain population growth. In the African Rift Valley, cities such as Bujumbura and Bukavu have expanded rapidly and informally into steep and unstable terrain amid political instability, displacement, and limited planning capacity [29, 61, 62]. In the Ethiopian Highlands, steep terrain coincides with rapid population growth, erratic rainfall, limited flat land, and livelihoods that remain strongly dependent on climate-sensitive agriculture [63–65]. In southern Yemen, conflict, repeated flash floods, and institutional disruption have contributed to informal settlement growth in areas where hazard monitoring and land governance are limited [66, 67]. In Afghanistan and northern Pakistan, populations in the Hindu Kush face landslides alongside earthquakes, floods, conflict, land scarcity, and limited infrastructure or emergency response [9, 56, 68–70].

However, steep-terrain population growth is not limited to conflict-affected or institutionally fragile regions. Eastern China provides a contrasting case, where steep-terrain population has increased alongside rapid economic development and greater institutional capacity. Changing rainfall extremes may alter landslide-triggering conditions [26], while urbanisation and infrastructure expansion increase the population and assets located near steep terrain [71–73]. Thus, similar patterns of steep-terrain population growth can occur under very different socioeconomic and institutional conditions.

Thus, several pathways may contribute to steep-terrain population growth, including rapid urbanisation, informal development, agricultural dependence, conflict, land scarcity, displacement, and unequal access to safe and serviced land. The importance of individual pathways is likely to vary substantially among regions. This heterogeneity also helps explain why a single global relationship is unlikely to capture the processes underlying steep-terrain population growth [21]. Future work should aim to disentangle the relative importance of these mechanisms by integrating more consistent data on migration flows, land and housing markets, infrastructure access, agricultural land use change, and household-level settlement decisions. Combining such information with projected settlement growth, future rainfall extremes and temporally varying landslide susceptibility could further identify where demographic and physical changes are likely to converge.

We show that in many hotspots, population growth on steep terrain occurs where rapid settlement expansion intersects with wider socioeconomic and environmental constraints. Future exposure may therefore become increasingly concentrated in a limited set of rapidly changing regions, although the associated landslide conditions differ among them. Research priorities should include Sub-Saharan Africa and South Asia, particularly the Kivu Rift, parts of the Ethiopian Highlands, and the Hindu Kush, where growth on steep terrain can exceed that on non-steep terrain. Investment should focus on hazard and impact data, monitoring, local susceptibility assessment, early warning, institutional capacity, and understanding how settlement expansion changes exposure. Increasing population on steep and potentially landslide-prone terrain should therefore be treated as a sustainable-development and land-planning concern as well as a hazard concern [74, 75].

Materials

Spatial units and aggregation

We selected topographic catchments as the primary spatial units. They represent natural boundaries for hillslope processes and reduce artifacts introduced by political borders. We chose to operate at the HydroBASINS Level 5 catchment scale, which provides global polygon boundaries for medium-sized catchments (10,000 km^2 mean area) derived from HydroSHEDS flow accumulation data using hierarchical Pfafstetter coding [37].

We aligned all gridded datasets to a common 1 km analysis grid by nearest neighbour method to avoid altering original data artificially. We then aggregated pixel-level values to catchments by summing population counts and computing settlement class shares within each catchment. Key aggregation assumptions were: (i) gridded population represents average conditions within each pixel, and (ii) catchment-scale summaries capture broad exposure patterns while smoothing local heterogeneity.

Datasets

We quantified long-term population and settlement dynamics using the Global Human Settlement Layer (GHSL). We used population counts from GHS-POP [1975–2025, 1 km resolution, 5-year intervals; 35], chosen for its long temporal coverage, uniform methodology and compatibility with other GHSL products used in this study. The dataset redistributes census-based population counts onto a grid using built-up information for global comparability.

We characterised settlement structure using GHS-SMOD [(Settlement Model, 1975–2025, 1 km resolution; 40]. GHS-SMOD is produced within the same GHSL framework as GHS-POP, allowing joint analysis of population and settlement change on a common grid. GHS-SMOD classifies each grid cell into settlement categories based on the Degree of Urbanisation (DEGURBA) framework endorsed by the UN Statistical Commission. DEGURBA integrates population density, built-up density and spatial contiguity to produce globally comparable settlement classes. GHS-SMOD

classes used in this study are urban centre, dense urban, semi-dense urban, peri-urban, rural cluster, low-density rural and very low-density rural.

We characterised long-term land-use and land-cover change using the HILDA+ dataset [43] which provides globally consistent annual land-use/land-cover states at 0.01° spatial resolution. We used the 1975 and 2019 state layers and aligned them to the common 1-km Mollweide analysis grid using nearest-neighbour resampling to preserve the categorical classes. The analysis focused on four land-cover transitions relevant to rapidly changing inhabited landscapes: forest loss, cropland expansion, pasture expansion, and built-up expansion.

We assigned each catchment a climate zone using the IPCC Climate Zone Map [2019; 41]. This gridded dataset applies a standardized classification scheme to Climate Research Unit Time Series (CRU TS) monthly temperature and precipitation data [1901–2019; 76], defining 12 domains based on thermal (polar, boreal, cool temperate, warm temperate, tropical), moisture (wet, moist, dry) and elevation (montane) regimes. We used this classification because it provides a compact set of global climate domains that supports clear cross-region comparison. The dataset contains 12 climate classes: Tropical Montane, Tropical Wet, Tropical Moist, Tropical Dry, Warm Temperate Moist, Warm Temperate Dry, Cool Temperate Moist, Cool Temperate Dry, Boreal Moist, Boreal Dry, Polar Moist and Polar Dry. We labelled each catchment by the dominant climate class within its boundary. This approach assumes that catchments with mixed climate coverage can be represented by their dominant class. Mixed-climate catchments therefore introduce some boundary uncertainty. Alternative climate classifications are possible, for example Köppen–Geiger, but the IPCC classification uses fewer classes and is better suited to the broad comparative focus of our analysis and compatibility of our results with future IPCC reports.

We used the global landslide-susceptibility map of Stanley and Kirschbaum [38] to evaluate the physical relevance of the slope-based terrain definition. The dataset provides global susceptibility classes at approximately 1-km resolution and combines information on slope, geology, faults, roads, and forest loss using a heuristic fuzzy-logic approach. Susceptibility is represented by five classes: Very Low, Low, Moderate, High, and Very High. We aligned the susceptibility raster to the common 1-km analysis grid using nearest-neighbour resampling to preserve the original categorical classes. We used the High and Very High classes as the primary comparison with terrain defined by slope $\geq 10°$.

To characterise potential rainfall-triggering conditions, we used intensity–duration–frequency (IDF) estimates from the BURGER dataset [39]. For each catchment, rainfall intensity was summarised using the 90th percentile of the BURGER grid cells intersecting the catchment. This captures relatively intense rainfall conditions within a catchment without relying on a single maximum grid-cell value. The rainfall metric is used only as an indicator of potential triggering conditions and not as a measure of landslide occurrence or frequency.

We used the 2024 World Bank Income Classification [2024; 77] to represent socioeconomic differences, assigning countries to low-, lower-middle-, upper-middle- or high-income groups. This classification provides a consistent global grouping for comparing exposure patterns. The 2024 classification used here includes 27 low-income,

55 lower-middle-income, 55 upper-middle-income and 61 high-income countries. We attributed each catchment to an income group using a population-weighted dominant-country approach. Specifically, we identified the country contributing most to the catchment's steep-slope population change and assigned that country's income group to the catchment.

To characterise institutional stability and conflict exposure in regions experiencing rapid steep-slope population growth, we used the World Bank Worldwide Governance Indicators (WGI), specifically the Political Stability and Absence of Violence/Terrorism percentile rank (1996–2024) [78]. In this metric, lower ranks indicate lower political stability across countries. We linked WGI rankings to catchments using the same population-weighted dominant-country approach as above to ensure consistency with the income-group attribution.

Terrain steepness and definition of 'steep'

Terrain steepness was obtained from GEOMORPHO90's 250m slope layers [36], derived from the globally consistent and hydrologically conditioned MERIT-DEM [79]. We selected GEOMORPHO90 over other raw terrain products because it provides a standardised, corrected surface suitable for our analysis. Although 90m layers are available as supplemental products, we used the 250m release because it is the primary global distribution with uniform preprocessing. We conducted the analysis at 1 km because a global, multi-decadal workflow at this resolution provides an efficient compromise that captures broad exposure patterns, while still being computationally feasible. We resampled the slope layer to 1 km using maximum aggregation, ensuring that steep terrain was preserved when matching the GHSL grid.

We defined steep terrain as slope $\geq 10°$. Slope is a primary control on landslide susceptibility [e.g., 31, 34, 38, 80], but no single slope threshold provides a complete representation of landslide-prone terrain globally. We therefore use the $10°$ threshold as a globally consistent first-order screening definition of steep terrain rather than as a landslide-susceptibility or hazard threshold. The purpose of the fixed threshold is to allow the same terrain definition to be applied consistently to the full 1975–2025 population series and across all regions. We calculated steep-slope population by masking the population rasters to pixels with slope $\geq 10°$ and summing within each catchment. The sensitivity of the results to this definition was evaluated using alternative slope thresholds, and its correspondence with independently mapped landslide susceptibility was assessed separately.

Robustness and sensitivity analyses

We assessed slope-threshold sensitivity by repeating key analyses using alternative slope thresholds ($8°$, $10°$, $12°$ and $15°$) to evaluate how results depend on the definition of 'steep' (Supplement Section 12). As expected, the exposed share declines for all income groups as the threshold is tightened. However, the ranking and separation between groups remain similar across thresholds. Hence, the income-group pattern is not dependent on the specific choice of the cutoff. We also compared the $\geq 10°$ threshold with the Stanley and Kirschbaum landslide-susceptibility classes (Supplement

Section S9). The $\geq 10^\circ$ threshold captured about 97% of High–Very High susceptibility terrain and about 86–88% of the associated positive population growth. Conversely, about 45% of slope-defined terrain and 47% of positive steep-terrain growth occurred within the High and Very High classes.

To test whether this affected hotspot identification, we independently ranked catchments by positive population growth on terrain $\geq 10^\circ$ and within High–Very High susceptibility terrain. 39 of the top 50 catchments were shared, and the rankings were strongly correlated (Spearman $\rho = 0.87$).

We further examined the physical context of the 50 largest absolute steep-terrain population-growth hotspots using the BURGER rainfall metric and mapped susceptibility (Supplement Section S10). Rainfall was represented by the catchment 90th percentile of 6-hour, 100-year intensity, while susceptibility was represented by the proportion of steep terrain classified as High or Very High. Forty-seven of the 50 hotspots had above-median rainfall intensity, 46 had above-median susceptibility, and 43 were above both medians.

We assessed robustness to population data choice by repeating our steep-slope population growth analysis with WorldPop and comparing it with GHS-POP over the overlap period 2000–2020 (Supplement Section S11).

We measured agreement between the two datasets by correlating the catchment rankings of positive steep-slope population growth on terrain $\geq 10^\circ$ using Spearman's rank correlation coefficient (ρ). We obtained a rank correlation of $\rho = 0.79$, indicating similar identification of high-growth catchments despite differences in population modelling inputs and methods. We also compared hotspot overlap using the top 50 catchments by positive steep-slope growth: 40 catchments overlapped, with 10 WorldPop-only and 10 GHS-only catchments.

The non-overlapping catchments were generally located near overlapping catchments within the same broader hotspot regions. These differences in individual catchment rankings may reflect differences in census harmonisation and population redistribution methods between the two datasets [60]. Nevertheless, both datasets identified similar broad geographic patterns of steep-terrain population growth.

Software and Implementation

All data processing and analysis were performed using Python 3.12.3.

Supplementary information. Supplementary information is available for this paper.

Acknowledgements. CG and TW acknowledge support from the Alexander von Humboldt Foundation in the framework of the Alexander von Humboldt Professorship endowed by the German Federal Ministry of Education and Research (BMBF).

UO is funded by the European Union (ERC, UrbanSlide, Grant 101160656, Doi: 10.3030/101160656). Views and opinions expressed are, however, those of the author(s) only and do not necessarily reflect those of the European Union or the European Research Council. Neither the European Union nor the granting authority can be held responsible for them.

Author contributions. All authors designed the study. C.G. performed the analyses and drafted the manuscript. U.O. and T.W. provided guidance and edited the manuscript and figures. The authors declare no competing interests.

References

[1] Pesaresi, M. *et al.* Atlas of the Human Planet 2017: Global Exposure to Natural Hazards. Tech. Rep. KJ-NA-28556-EN-N (online),KJ-NA-28556-EN-C (print),KJ-NA-28556-EN-E (ePub), Joint Research Centre, Luxembourg (Luxembourg) (2017).

[2] IDMC. Global Report on Internal Displacement. Tech. Rep., Internal Displacement Monitoring Centre (2025).

[3] UNHCR. No Escape II: The Way Forward. Bringing climate solutions to the frontlines of conflict and displacement. Tech. Rep., United Nations High Commissioner for Refugees (2025). URL https://www.unhcr.org/media/no-escape-ii-way-forward.

[4] Emmer, A. Geographies and Scientometrics of Research on Natural Hazards. *Geosciences 2018, Vol. 8, Page 382* **8**, 382 (2018). URL https://www.mdpi.com/2076-3263/8/10/382/htmhttps://www.mdpi.com/2076-3263/8/10/382.

[5] Stein, L. *et al.* Wealth Over Woe: Global Biases in Hydro-Hazard Research. *Earth's Future* **12**, e2024EF004590 (2024). URL /doi/pdf/10.1029/2024EF004590https://onlinelibrary.wiley.com/doi/abs/10.1029/2024EF004590https://agupubs.onlinelibrary.wiley.com/doi/10.1029/2024EF004590.

[6] Ferrer, J. V. *et al.* Human Settlement Pressure Drives Slow-Moving Landslide Exposure. *Earth's Future* **12**, e2024EF004830 (2024). URL /doi/pdf/10.1029/2024EF004830https://onlinelibrary.wiley.com/doi/abs/10.1029/2024EF004830https://agupubs.onlinelibrary.wiley.com/doi/10.1029/2024EF004830.

[7] Field, C. B. *et al.* Technical summary Climate Change 2014: Impacts, Adaptation, and Vulnerability. Part A: Global and Sectoral Aspects. Contribution of Working Group II to the Fifth Assessment Report of the Intergovernmental Panel on Climate Change ed CB Field et al. *Climate Change* **2014**, 35–94 (2014).

[8] Oppenheimer, M. *et al.* Emergent risks and key vulnerabilities Climate Change 2014: Impacts, Adaptation, and Vulnerability. Part A: Global and Sectoral Aspects. Contribution of Working Group II to the Fifth Assessment Report of the Intergovernmental Panel on Climate Change ed CB Field et al. *Cambridge UK, and New York:[sn]* (2014).

[9] Dilley, M. *et al.* Natural disaster hotspots: A global risk analysis. *World Bank Disaster Risk Management Series* **5**, 1–132 (2005).

[10] Froude, M. J. & Petley, D. N. Global fatal landslide occurrence from 2004 to 2016. *Natural Hazards and Earth System Sciences* **18**, 2161–2181 (2018).

[11] Delforge, D. *et al.* EM-DAT: the Emergency Events Database. *International Journal of Disaster Risk Reduction* **124**, 105509 (2025). URL https://www.sciencedirect.com/science/article/pii/S2212420925003334?via%3Dihub.

[12] Nadim, F., Kjekstad, O., Peduzzi, P., Herold, C. & Jaedicke, C. Global landslide and avalanche hotspots. *Landslides 2006 3:2* **3**, 159–173 (2006). URL https://link.springer.com/article/10.1007/s10346-006-0036-1.

[13] Fidan, S. *et al.* Understanding fatal landslides at global scales: a summary of topographic, climatic, and anthropogenic perspectives. *Natural Hazards 2024 120:7* **120**, 6437–6455 (2024). URL https://link.springer.com/article/10.1007/s11069-024-06487-3.

[14] Gariano, S. L. & Guzzetti, F. Landslides in a changing climate. *Earth-Science Reviews* **162**, 227–252 (2016). URL https://www.sciencedirect.com/science/article/pii/S0012825216302458#section-cited-by.

[15] Schillerberg, T. A. & Tian, D. Global Assessment of Compound Climate Extremes and Exposures of Population, Agriculture, and Forest Lands Under Two Climate Scenarios. *Earth's Future* **12**, e2024EF004845 (2024). URL /doi/pdf/10.1029/2024EF004845https://onlinelibrary.wiley.com/doi/abs/10.1029/2024EF004845https://agupubs.onlinelibrary.wiley.com/doi/10.1029/2024EF004845.

[16] Stalhandske, Z. *et al.* Global assessment of population exposure to multiple climate-related hazards from 2003 to 2021: a retrospective analysis. *The Lancet Planetary Health* **9**, 101295 (2025). URL https://www.sciencedirect.com/science/article/pii/S2542519625001731?via%3Dihub#sec2.

[17] Fidan, S., Görüm, T., Akbaş, A., Ekberzade, B. & Ozturk, U. Wealth and land-cover change govern landslide fatalities on world's mountains. *Science Advances* **12**, eaec2739 (2026).

[18] Ferrer, J. V. *et al.* Exposure to Large Landslides in Cities Outpaces Urban Growth. *Geophysical Research Letters* **52**, e2025GL115170 (2025). URL /doi/pdf/10.1029/2025GL115170https://onlinelibrary.wiley.com/doi/abs/10.1029/2025GL115170https://agupubs.onlinelibrary.wiley.com/doi/10.1029/2025GL115170.

[19] Shi, K., Cui, Y., Liu, S. & Wu, Y. Global Urban Land Expansion Tends To Be Slope Climbing: A Remotely Sensed Nighttime Light Approach. *Earth's*

Future **11**, e2022EF003384 (2023). URL /doi/pdf/10.1029/2022EF003384https://onlinelibrary.wiley.com/doi/abs/10.1029/2022EF003384https://agupubs.onlinelibrary.wiley.com/doi/10.1029/2022EF003384.

[20] Emberson, R., Kirschbaum, D. & Stanley, T. New global characterisation of landslide exposure. *Natural Hazards and Earth System Sciences* **20**, 3413–3424 (2020).

[21] Alcántara-Ayala, I. Landslides in a changing world. *Landslides* **22**, 2851–2865 (2025).

[22] Fowler, H. J. *et al.* Anthropogenic intensification of short-duration rainfall extremes. *Nature Reviews Earth & Environment 2021 2:2* **2**, 107–122 (2021). URL https://www.nature.com/articles/s43017-020-00128-6.

[23] Calvin, K. *et al.* IPCC, 2023: Climate Change 2023: Synthesis Report. Contribution of Working Groups I, II and III to the Sixth Assessment Report of the Intergovernmental Panel on Climate Change [Core Writing Team, H. Lee and J. Romero (eds.)]. IPCC, Geneva, Switzerland. Tech. Rep., Intergovernmental Panel on Climate Change (2023).

[24] Duan, Y. *et al.* Global projections of future landslide susceptibility under climate change. *Geoscience Frontiers* **16**, 102074 (2025). URL https://www.sciencedirect.com/science/article/pii/S1674987125000799#b0275.

[25] Kirschbaum, D., Kapnick, S. B., Stanley, T. & Pascale, S. Changes in Extreme Precipitation and Landslides Over High Mountain Asia. *Geophysical Research Letters* **47**, e2019GL085347 (2020). URL /doi/pdf/10.1029/2019GL085347https://onlinelibrary.wiley.com/doi/abs/10.1029/2019GL085347https://agupubs.onlinelibrary.wiley.com/doi/10.1029/2019GL085347.

[26] Lin, Q. *et al.* Evaluation of potential changes in landslide susceptibility and landslide occurrence frequency in China under climate change. *Science of The Total Environment* **850**, 158049 (2022). URL https://www.sciencedirect.com/science/article/pii/S0048969722051488?pes=vor&utm_source=iopp&getft_integrator=iopp#f0025.

[27] Bozzolan, E. *et al.* A mechanistic approach to include climate change and unplanned urban sprawl in landslide susceptibility maps. *Science of the total environment* **858**, 159412 (2023).

[28] Ullah, K. *et al.* Spatiotemporal dynamics of landslide susceptibility under future climate change and land use scenarios. *Environmental Research Letters* **19**, 124016 (2024). URL https://iopscience.iop.org/article/10.1088/1748-9326/ad8a72https://iopscience.iop.org/article/10.1088/1748-9326/ad8a72/meta.

[29] Depicker, A. *et al.* Historical dynamics of landslide risk from population and forest-cover changes in the Kivu Rift. *Nature Sustainability 2021 4:11* **4**, 965–974 (2021). URL https://www.nature.com/articles/s41893-021-00757-9.

[30] Bozzolan, E., Holcombe, E., Pianosi, F. & Wagener, T. Including informal housing in slope stability analysis–an application to a data-scarce location in the humid tropics. *Natural Hazards and Earth System Sciences* **20**, 3161–3177 (2020).

[31] Ozturk, U. *et al.* How climate change and unplanned urban sprawl bring more landslides. *Nature 2022 608:7922* **608**, 262–265 (2022). URL https://www.nature.com/articles/d41586-022-02141-9.

[32] Cutter, S. L., Boruff, B. J. & Shirley, W. L. Social Vulnerability to Environmental Hazards*. *Social Science Quarterly* **84**, 242–261 (2003). URL /doi/pdf/10.1111/1540-6237.8402002https://onlinelibrary.wiley.com/doi/abs/10.1111/1540-6237.8402002https://onlinelibrary.wiley.com/doi/10.1111/1540-6237.8402002.

[33] Serwajja, E., Kisira, Y. & Bamutaze, Y. 'better to die of landslides than hunger': Socio-economic and cultural intricacies of resettlement due to climate-induced hazards in uganda. *International Journal of Disaster Risk Reduction* **101**, 104242 (2024). URL https://www.sciencedirect.com/science/article/pii/S2212420924000049.

[34] Reichenbach, P., Rossi, M., Malamud, B. D., Mihir, M. & Guzzetti, F. A review of statistically-based landslide susceptibility models. *Earth-Science Reviews* **180**, 60–91 (2018). URL https://www.sciencedirect.com/science/article/pii/S0012825217305652.

[35] Schiavina M., Freire S., Carioli A. & MacManus K. GHS-POP R2023A - GHS population grid multitemporal (1975-2030) (2023).

[36] Amatulli, G., McInerney, D., Sethi, T., Strobl, P. & Domisch, S. Geomorpho90m, empirical evaluation and accuracy assessment of global high-resolution geomorphometric layers. *Scientific Data 2020 7:1* **7**, 162– (2020). URL https://www.nature.com/articles/s41597-020-0479-6.

[37] Lehner, B. & Grill, G. Global river hydrography and network routing: Baseline data and new approaches to study the world's large river systems. *Hydrological Processes* **27**, 2171–2186 (2013). URL /doi/pdf/10.1002/hyp.9740https://onlinelibrary.wiley.com/doi/abs/10.1002/hyp.9740https://onlinelibrary.wiley.com/doi/10.1002/hyp.9740.

[38] Stanley, T. & Kirschbaum, D. B. A heuristic approach to global landslide susceptibility mapping. *Natural hazards* **87**, 145–164 (2017).

[39] Hoch, J. *et al.* Burger - a bottom-up regionalization approach for global sub-daily intensity-duration-frequency data (2025). URL https://doi.org/10.5281/zenodo.

15473689.

[40] Schiavina M., Melchiorri M. & Pesaresi M. GHS-SMOD R2023A - GHS settlement layers, application of the Degree of Urbanisation methodology (stage I) to GHS-POP R2023A and GHS-BUILT-S R2023A, multitemporal (1975-2030) (2023).

[41] IPCC. Ipcc-national greenhouse gas inventories (tfi) (2019). URL https://www.ipcc-nggip.iges.or.jp/public/2019rf/corrigenda1.html.

[42] Dewitte, O. *et al.* Constraining landslide timing in a data-scarce context: from recent to very old processes in the tropical environment of the North Tanganyika-Kivu Rift region. *Landslides 2020 18:1* **18**, 161–177 (2020). URL https://link.springer.com/article/10.1007/s10346-020-01452-0.

[43] Winkler, K., Fuchs, R., Rounsevell, M. & Herold, M. Global land use changes are four times greater than previously estimated. *Nature Communications 2021 12:1* **12**, 2501– (2021). URL https://www.nature.com/articles/s41467-021-22702-2.

[44] Nieto, S., Aristizábal, E. & Ozturk, U. Coupled evolution of a city and landslides. *Environmental Research Letters* **20**, 054001 (2025). URL https://iopscience.iop.org/article/10.1088/1748-9326/adc4d8https://iopscience.iop.org/article/10.1088/1748-9326/adc4d8/meta.

[45] Gall, M., Borden, K. A. & Cutter, S. L. When do losses count? six fallacies of natural hazards loss data. *Bulletin of the American Meteorological Society* **90**, 799–810 (2009).

[46] Zhu, Y. *et al.* Landslide susceptibility assessment and attribution analysis in yunnan province based on weighted information value-logistic regression model. *Geomatics, Natural Hazards and Risk* **16**, 2525428 (2025).

[47] Chowdhury, M. S. *et al.* Gis-based landslide susceptibility mapping using logistic regression, random forest and decision and regression tree models in chattogram district, bangladesh. *Heliyon* **10** (2024).

[48] Ali, S., Biermanns, P., Haider, R. & Reicherter, K. Landslide susceptibility mapping by using a geographic information system (gis) along the china–pakistan economic corridor (karakoram highway), pakistan. *Natural Hazards and Earth System Sciences* **19**, 999–1022 (2019).

[49] Bozzolan, E., Holcombe, E., Pianosi, F. & Wagener, T. Synthetic libraries of urban landslide simulations to identify slope failure hotspots and drivers across spatial scales and landscapes. *Landslides* **22**, 637–654 (2025).

[50] Ravetz, J. & Sahana, M. Where is the peri-urban? Mapping the areas 'around, beyond and between'. *Frontiers in Sustainable Cities* **7**, 1436287 (2025).

[51] Maricato, E. The Future of Global Peripheral Cities. *Latin American Perspectives* **44**, 18–37 (2017). URL /doi/pdf/10.1177/0094582X16685174?download=true.

[52] Sepúlveda, S. A. & Petley, D. N. Regional trends and controlling factors of fatal landslides in Latin America and the Caribbean. *Hazards Earth Syst. Sci* **15**, 1821–1833 (2015). URL http://geonames.nga.

[53] Nsabimana, J. *et al.* Geo-Hydrological Hazard Impacts, Vulnerability and Perception in Bujumbura (Burundi): A High-Resolution Field-Based Assessment in a Sprawling City. *Land 2023, Vol. 12,* **12** (2023). URL https://www.mdpi.com/2073-445X/12/10/1876.

[54] Lavell, A., Chávez Eslava, A., Barros Salas, C. & Miranda Sandoval, D. Inequality and the social construction of urban disaster risk in multi-hazard contexts: the case of Lima, Peru and the COVID-19 pandemic. *Environment and Urbanization* **35**, 131–155 (2023). URL https://journals.sagepub.com/doi/10.1177/09562478221149883.

[55] Bastos Moroz, C. & Thieken, A. H. Urban growth and spatial segregation increase disaster risk: lessons learned from the 2023 disaster on the North Coast of São Paulo, Brazil. *Natural Hazards and Earth System Sciences* **24**, 3299–3314 (2024). URL https://nhess.copernicus.org/articles/24/3299/2024/.

[56] Witze, A. Afghan landslide was 'an accident waiting to happen'. *Nature 2014* (2014). URL https://www.nature.com/articles/nature.2014.15158.

[57] Zaid, H. A. H., Jamaluddin, T. A. & Arifin, M. H. Overview of slope stability, earthquakes, flash floods and expansive soil hazards in the republic of yemen. *Bulletin of the Geological Society of Malaysia* **71**, 71–78 (2021).

[58] Hsiang, S. M., Meng, K. C. & Cane, M. A. Civil conflicts are associated with the global climate. *Nature 2011 476:7361* **476**, 438–441 (2011). URL https://www.nature.com/articles/nature10311.

[59] Mora, C. *et al.* Broad threat to humanity from cumulative climate hazards intensified by greenhouse gas emissions. *Nature Climate Change 2018 8:12* **8**, 1062–1071 (2018). URL https://www.nature.com/articles/s41558-018-0315-6.

[60] Thornton, J. M. *et al.* Human populations in the world's mountains: Spatio-temporal patterns and potential controls. *PLOS ONE* **17**, e0271466 (2022). URL https://journals.plos.org/plosone/article?id=10.1371/journal.pone.0271466.

[61] Depicker, A. *et al.* Mobilization rates of landslides in a changing tropical environment: 60-year record over a large region of the East African Rift. *Geomorphology* **454**, 109156 (2024). URL https://www.sciencedirect.com/science/article/pii/S0169555X24001065?via%3Dihub.

[62] Dille, A. *et al.* Acceleration of a large deep-seated tropical landslide due to urbanization feedbacks. *Nature Geoscience 2023 15:12* **15**, 1048–1055 (2022). URL https://www.nature.com/articles/s41561-022-01073-3.

[63] Abebe, B., Dramis, F., Fubelli, G., Umer, M. & Asrat, A. Landslides in the Ethiopian highlands and the Rift margins. *Journal of African Earth Sciences* **56**, 131–138 (2010). URL https://www.sciencedirect.com/science/article/pii/S1464343X09001113?via%3Dihub.

[64] EEA. Report on the Ethiopian Economy: Economic Performance and Governance in Ethiopia. Tech. Rep., Ethiopian Economics Association (2025). URL https://eea-et.org/publication/report-on-the-ethiopian-economy-2025_economic-performance-and-governance-in-ethiopia/.

[65] GCR. Ethiopia in Crisis: Deadly Landslides and the Growing Climate Threat (2025). URL https://globalclimaterisks.org/insights/blog/ethiopia-in-crisis-deadly-landslides-and-the-growing-climate-threat/.

[66] IDMC. Yemen — IDMC - Internal Displacement Monitoring Centre (2025). URL https://www.internal-displacement.org/countries/yemen/.

[67] IOM. Report on Migration, Environment and Climate Change in Yemen. Tech. Rep., International Organization for Migration (IOM), UN Migration (2023).

[68] Rusk, J. *et al.* Multi-hazard susceptibility and exposure assessment of the Hindu Kush Himalaya. *Science of The Total Environment* **804**, 150039 (2022). URL https://www.sciencedirect.com/science/article/pii/S0048969721051147#bb0100.

[69] Ruttig, T. Slippery Slopes: Ecological, social and developmental aspects of the Badakhshan landslide disaster (2014). URL https://www.afghanistan-analysts.org/en/reports/economy-development-environment/slippery-slopes-ecological-social-and-developmental-aspects-of-the-badakhshan-landslide-disaster/.

[70] Salehzada, H., Qasimi, M. & Rezayi, S. Landslide in Badakhshan, Afghanistan (2014). URL https://www.adpc.net/igo/contents/iPrepare/iprepare-news_id.asp?ipid=250.

[71] Tong, B. *et al.* The corresponding countermeasures of landslide risk control under influence of climate change in China. *Geomatics, Natural Hazards and Risk* **15** (2024). URL https://www.tandfonline.com/doi/pdf/10.1080/19475705.2024.2421387.

[72] GFDRR. Learning from Experience Insights from China's Progress in Disaster Risk Management Learning from Experience. Tech. Rep., The World Bank (2020). URL www.worldbank.org.

[73] Zhou, L., Wu, X., Ji, Z. & Gao, G. Characteristic analysis of rainstorm-induced catastrophe and the countermeasures of flood hazard mitigation about Shenzhen city. *Geomatics, Natural Hazards and Risk* **8**, 1886–1897 (2017). URL https://www.tandfonline.com/doi/pdf/10.1080/19475705.2017.1392368.

[74] Kelman, I. Linking disaster risk reduction, climate change, and the sustainable development goals. *Disaster Prevention and Management* **26**, 254–258 (2017). URL https://dx.doi.org/10.1108/DPM-02-2017-0043.

[75] Parsons, M. *et al.* Critical science for the next decade of climate risk management. *Climate Risk Management* 100770 (2025). URL https://linkinghub.elsevier.com/retrieve/pii/S2212096325000841.

[76] Harris, I., Osborn, T. J., Jones, P. & Lister, D. Version 4 of the cru ts monthly high-resolution gridded multivariate climate dataset. *Scientific data* **7**, 109 (2020).

[77] Fantom, N. J. & Serajuddin, U. The World Bank's classification of countries by income. *Policy Research Working Paper Series* (2016). URL https://ourworldindata.org/grapher/world-bank-income-groups.

[78] World bank, worldwide governance indicators (2024). URL https://www.worldbank.org/en/publication/worldwide-governance-indicators.

[79] Yamazaki, D. *et al. Merit dem: A new high-accuracy global digital elevation model and its merit to global hydrodynamic modeling*, Vol. 2017, H12C–04 (2017).

[80] Triplett, L. D. *et al.* Factors influencing landslide occurrence in low-relief formerly glaciated landscapes: landslide inventory and susceptibility analysis in minnesota, usa. *Natural Hazards* **121**, 11799–11827 (2025).